

On the possibility of exploring tip-molecule interactions with STM experiments

Christoph Schiel, Philipp Rahe, and Philipp Maass
*Fachbereich Physik, Universität Osnabrück, Germany**
(Dated: August 1, 2022)

We present a theory for analyzing residence times of single molecules in a fixed detection area of a scanning tunneling microscope (STM). The approach is developed for one-dimensional molecule diffusion and can be extended to two dimensions by using the same methodology. Explicit results are derived for a harmonic attractive and repulsive tip-molecule interaction. Applications of the theory allows one to estimate the type and strength of interactions between the STM tip and the molecule. This includes the possibility of an estimation of molecule-molecule interaction when the tip is decorated by a molecule. Despite our focus on STM, this theory can analogously be applied to other experimental probes that monitor single molecules.

I. INTRODUCTION

For controlling the kinetic growth and self-assembly of molecules on surfaces, the molecular diffusion coefficient is one important parameter [1]. Multiple methods have been developed to obtain this parameter [2]. Here we focus on a specific technique of determining the diffusion coefficient from the analysis of current fluctuations in scanning tunneling microscopy (STM). These fluctuations are caused by molecules entering and leaving the detection area under an STM tip at a fixed spatial position [3–6]. Thus, this method is particularly well suited for molecules with high mobility since the tunneling current can be measured at a high time resolution. It can also be applied in other fields as, for example, fluorescence correlation spectroscopy [7–11].

In previous studies, different techniques have been developed and investigated to evaluate the times series of the tunneling current [5, 6]. These studies include molecules of different shapes, as well as effects of additional rotational diffusion. With an appropriate analysis, the time series of the tunneling current can be mapped onto a binary signal (dichotomic fluctuations), where the signal value is one for a molecule under the tip and zero otherwise, see Fig. 1 for an example of the resulting rectangular peaks.

The stochastic behavior of the binary signal can be characterized by two characteristic times, namely the residence time and the interpeak time. The residence time is the duration of a rectangular peak and the interpeak time is the time interval between two consecutive rectangular peaks. By sampling these times in a long time series, a residence time distribution (RTD) and an interpeak time distribution (ITD) are obtained. Based on theoretical modeling without tip-molecule interactions, these measured distributions can be fitted to analytical

predictions and diffusion coefficients are extracted as fitting parameters. As a third approach, the experimentally determined autocorrelation function (ACF) of the signal is compared with theoretical expressions.

The ITD is governed by the diffusive dynamics of the molecules while they are outside the detection area of the tip. Accordingly, tip-molecule interactions does not influence the diffusion coefficient under the assumption that the tip-molecule interaction range is shorter or equal to the detection range. This is in marked contrast to the RTD, where the diffusive dynamics is examined while a molecule is located in the tip-sample gap. This contrasting behavior can be exploited to probe tip-molecule interactions by modeling the influence of these interactions on the diffusion coefficient. This could become an interesting new technique for analyzing molecule-molecule interactions beyond current methods such as atomic force microscopy, in particular in view of the possibility to decorate STM tips with specific molecules. Comparison of

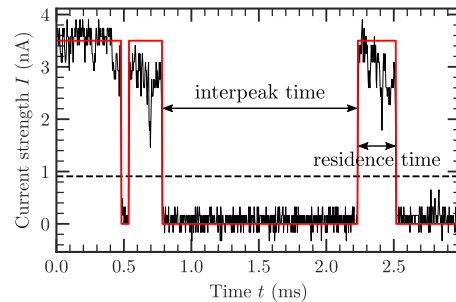


FIG. 1. Typical tunneling current measured with an STM. In this example, the fluctuations by diffusing PTCDA (perylene-tetracarboxylic dianhydride) molecules on the Ag(110) surface are sampled. The black line is the measured current. The dotted line indicates the threshold value. Currents above this threshold are caused by the presence of PTCDA molecules under the tip. The red line indicates the resulting dichotomic fluctuations of the current (binary signal). The width of a rectangular peak in the binary representation gives the residence time. The time between the termination and start of two consecutive rectangular peaks gives the interpeak time.

* maass@uni-osnabrueck.de

ITDs and RDTs measured in one experiment can thus become a valuable tool for analyzing molecule-molecule interactions. The ACF approach would be not suitable for such analysis because both the diffusion inside and outside the detection area under the tip enter its functional behavior.

Here, we perform first steps to evaluate this idea of quantifying tip-molecule interactions via their influence on diffusion coefficients. To this end, we present a theory for the RTD in the presence of a harmonic interaction between tip and molecule. Using this theory, we evaluate how such interactions modify the RTD for a freely diffusing molecule on the surface. This includes both attractive and repulsive interactions with the tip.

II. RESIDENCE TIME DISTRIBUTION IN THE PRESENCE OF TIP-MOLECULE INTERACTION: GENERAL FORMAL SOLUTION

We focus on a one-dimensional diffusion of the molecules on the surface, which allows us to obtain explicit analytical expressions. A one-dimensional treatment can also be appropriate to describe experimental situations of highly anisotropic molecule diffusion, as it is encountered, for example, on (110) surfaces.

To be specific, we consider the diffusion of a molecule at a temperature T under a tip pointing to the origin of the coordinate frame. The tip-molecule interaction is described by $V(x) = V(-x)$, where x is the center of the molecule. The detection interval of the molecule under the tip is $[-L/2, L/2]$, corresponding to a spacial tip-molecule interaction range of $L/2$. In the absence of tip-molecule interaction ($V(x) = 0$), the molecule diffusion coefficient is D_0 .

The residence time is the time between the event where a molecule center enters the detection interval and the event where it leaves that interval thereafter. Accordingly, the RTD is equal to a first-passage time distribution. This distribution follows from the probability $p(x, t)dx$ of finding the molecule in the interval $[x, x + dx]$ under the conditions that absorbing boundaries are present at $-L/2$ and $L/2$,

$$p(-L/2, t) = p(L/2, t) = 0. \quad (1)$$

The initial molecule position $p(x, 0)$ at time $t = 0$ is $-L/2 + \epsilon$ (or $L/2 - \epsilon$) where ϵ is a small displacement away from the absorbing boundary. Accordingly, we can set

$$p(x, 0) = \frac{1}{2} [\delta(x + (L/2 - \epsilon)) + \delta(x - (L/2 - \epsilon))]. \quad (2)$$

We take ϵ as the root mean squared displacement of a freely diffusing molecule within the time resolution interval Δt of the time series, $\epsilon = \sqrt{D_0 \Delta t}$. The first-passage

time distribution or RTD is given by [12]

$$\Psi(t) = -\frac{\partial}{\partial t} \int_{-L/2}^{L/2} p(x, t), \quad (3)$$

where $p(x, t)$ is the probability density for the initial condition (2) and absorbing boundary condition (1). Its time evolution is given by the diffusion equation [13]

$$\frac{\partial p(x, t)}{\partial t} = L_s(x)p(x, t), \quad (4)$$

where

$$L_s(x) = D_0 \left[\frac{\partial^2}{\partial x^2} - \beta \frac{\partial}{\partial x} V'(x) \right] \quad (5)$$

is the Smoluchowski time evolution operator; $\beta = 1/k_B T$ is the inverse thermal energy.

A general formal solution of Eq. (4) can be obtained by introducing the self-adjoint operator [13],

$$\begin{aligned} L(x) &= e^{\beta V(x)/2} L_s(x) e^{-\beta V(x)/2} \\ &= D_0 \left[\frac{\partial^2}{\partial x^2} + \frac{\beta}{2} V''(x) - \frac{\beta^2}{4} V'(x)^2 \right], \end{aligned} \quad (6)$$

which is the time evolution operator for the rescaled probability density $e^{\beta V(x)/2} p(x, t)$. The solution for $p(x, t)$ is

$$p(x, t) = e^{-\beta V(x)/2} \sum_n a_n \varphi_n(x) e^{-\lambda_n t} \quad (7)$$

where

$$a_n = \int_{-L/2}^{L/2} \varphi_n(x) e^{\beta V(x)/2} p(x, 0) dx \quad (8)$$

and $\varphi_n(x)$ are the eigenfunctions of the operator $L(x)$,

$$L(x)\varphi_n(x) = -\lambda_n \varphi_n(x). \quad (9)$$

The eigenfunctions must satisfy the same boundary conditions (1) as $p(x, t)$,

$$\varphi(-L/2) = \varphi(L/2) = 0. \quad (10)$$

Inserting $p(x, t)$ from Eq. (7) in Eq. (3) gives

$$\Psi(t) = \sum_n a_n b_n \lambda_n e^{-\lambda_n t} \quad (11)$$

where

$$b_n = \int_{L/2}^{L/2} dx \varphi_n e^{-\beta V/2}. \quad (12)$$

Using this approach, the determination of the RTD reduces to a calculation of the eigenfunctions $\varphi(x)$.

In the non-interacting case $V(x) = 0$, Eq. (11) yields

$$\Psi_0 = \frac{4}{\pi\tau_L} \sum_{n=0}^{\infty} (2n+1) \sin\left(\frac{(2n+1)\pi\epsilon}{L}\right) e^{-(2n+1)^2 t/\tau_L}, \quad (13)$$

where

$$\tau_L = \frac{L^2}{\pi^2 D_0}. \quad (14)$$

It can be shown [5] that Eq. (13) gives a power law $\propto t^{-3/2}$ for $\Delta t \ll t \ll \tau_L$ and an exponential decay for $t \gg \tau_L$.

III. RESIDENCE TIME DISTRIBUTION FOR HARMONIC TIP-MOLECULE INTERACTION

Generally, a tip-molecule interaction can be of complex physical origin and include numerous contributions. For simplicity, we here consider a potential along the lateral position x of the harmonic form

$$V(x) = \begin{cases} V_0 - \frac{k}{2}x^2, & x \in [-L/2, L/2], \\ 0, & \text{otherwise} \end{cases} \quad (15)$$

with $V_0 = kL^2/8$, which makes the potential continuous at $x = \pm L/2$. The stiffness k is positive (negative) for repulsive (attractive) interaction.

The eigenvalue problem in Eq. (9) then reads

$$D_0 \left[\frac{d^2}{dx^2} - \frac{\beta k}{2} - \frac{\beta^2 k^2}{4} x^2 \right] \varphi_n(x) = \lambda_n \varphi_n(x) \quad (16)$$

in explicit form. Introducing the dimensionless length $y = \sqrt{\pm\beta k} x$ and defining $\tilde{\varphi}_n(y) = \varphi_n(x) = \varphi_n(y/\sqrt{\pm\beta k})$, we obtain the differential equation for parabolic cylinder functions [14],

$$\frac{d^2 \tilde{\varphi}_n(y)}{dy^2} - \left(\frac{1}{4} y^2 \pm c_n \right) \tilde{\varphi}_n(y) = 0. \quad (17)$$

Here and in the following the upper (lower) sign refers to repulsive (attractive) interaction, and

$$c_n = \frac{1}{2} - \frac{\lambda_n}{\beta k D_0}. \quad (18)$$

Due to the symmetry of the potential, the eigenfunctions $\tilde{\varphi}_n$ can be chosen to be eigenfunctions also of the parity operator. The fundamental system of solutions of Eq. (17) is thus given by even and odd solutions. The even solutions are

$$\tilde{\varphi}_n(y) = e^{-\frac{1}{4}y^2} M\left(\frac{1}{4} \pm \frac{c_n}{2}, \frac{1}{2}, \frac{1}{2}y^2\right), \quad (19)$$

where $M(\alpha, \gamma, z)$ is Kummer's confluent hypergeometric function. The odd solutions do not contribute to the

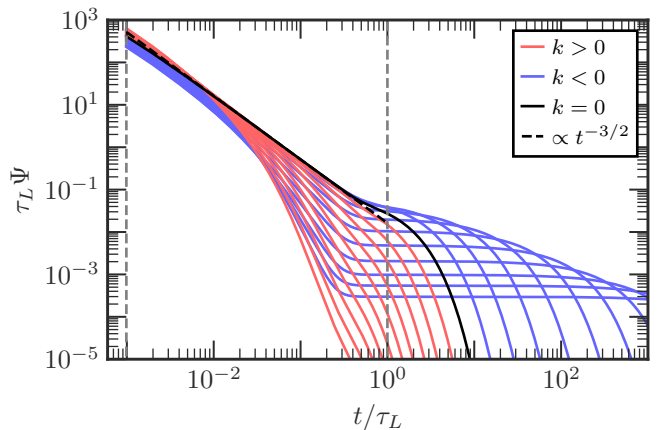


FIG. 2. Scaled residence time distributions $\tau_L \Psi$ for attractive (blue lines) and repulsive (red lines) interactions. The black line shows $\tau_L \Psi_0$ in the absence of tip-molecule interactions [see Eq. (13)]. In between the dashed gray lines that corresponds to the time interval between Δt (time resolution) and τ_L (see Eq. (14)), Ψ_0 decays as a power law, $\Psi_0 \sim t^{-3/2}$. The scaled stiffness $\beta k L^2$ is varied in steps of 10 from $\beta k L^2 = -100$ to 100 (with increasing $\beta|k|L^2$ the curves shift further away from the $\Psi_0(t)$ curve). The displacement ϵ entering the initial condition (2) is $\epsilon = 0.01L$.

RTD (11), because the respective a_n in Eq. (8) are zero for these odd solutions due to the symmetry of the potential and of the initial condition (2).

The c_n or corresponding eigenvalues λ_n [cf. Eq. (18)] follow from the boundary conditions in Eq. (10),

$$M\left(\frac{1}{2} \pm \frac{c_n}{2}, \frac{1}{2}, \pm \frac{\beta k L^2}{8}\right) = 0. \quad (20)$$

The eigenfunctions are

$$\varphi_n(x) = \mathcal{N}_n e^{\mp \beta k x^2/4} M\left(\frac{1}{2} \pm \frac{c_n}{2}, \frac{1}{2}, \pm \frac{\beta k x^2}{2}\right) \quad (21)$$

with normalization factor

$$\mathcal{N}_n = \left[\int_{-L/2}^{L/2} \varphi_n(x)^2 dx \right]^{-1}. \quad (22)$$

Figure 2 shows scaled RTDs $\tau_L \Psi$ as a function of t/τ_L for repulsive and attractive harmonic interactions of varying stiffness k . The black curve represents the RTD $\Psi_0(t)$ in the absence of tip-molecule interaction. As mentioned above, it decays as a power law $\sim t^{-3/2}$ for $\Delta t < t < \tau_L$ and exponentially for $t > \tau_L$.

For analyzing the impact of the tip-molecule interaction, RTDs in Fig 2 are displayed for scaled stiffnesses $\beta k L^2$ varied in steps of 10 from $\beta k L^2 = -100$ to 100 ($\beta k L^2 = \pm 10$ are the closest lines to the black curve representing the RTD Ψ_0 in the non-interacting case). For small stiffness, $\beta|k|L^2 \leq 10$, deviations from $\Psi_0(t)$ are mainly present in the exponential tail of the distribution, while they are hardly visible in the power law

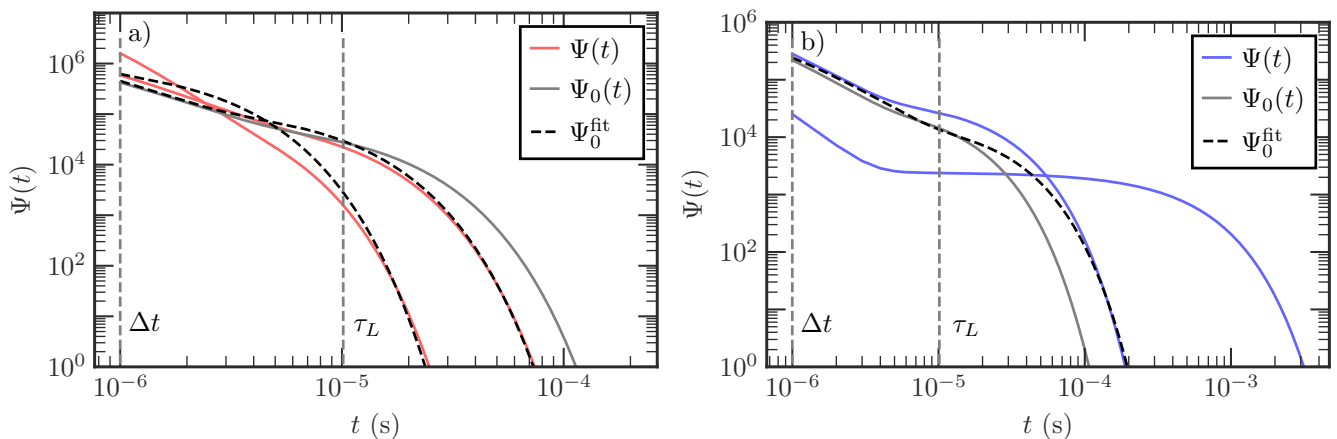


FIG. 3. Residence time distributions $\Psi(t)$ for (a) repulsive (red solid lines) and (b) attractive interactions (red solid lines) of two scaled stiffnesses $\beta kL^2 = \pm 10$ and $\beta kL^2 = \pm 50$. The gray solid lines shows the RTD $\Psi_0(t)$ in the absence of tip-molecule interaction. The curves representing Ψ_0^{fit} (dashed black lines) are fits of Eq. (13) to $\ln \Psi(t)$ with the method of least-squares, i.e. fits under the assumption that a tip-molecule interaction is not present. The results are shown for typical parameters estimated from the RTD analysis described in Ref. [5]: $D_0/L^2 = 10^4 \text{ s}^{-1}$ and $\epsilon/L = 0.1$. The dashed gray lines mark the time interval between Δt (time resolution) and τ_L [see Eq. (14)]. This interval is narrower here than in Fig. 2 due to the larger value of ϵ/L .

regime. With increasing $\beta|k|L^2$, deviations become more pronounced and can be seen also for small times $t < \tau_L$.

For the attractive interaction, the probability of a molecule to leave the detection interval at small times $t \ll \tau_L$ is reduced compared to $\Psi_0(t)$. For large times $t > \tau_L$, by contrast, it is strongly increased. This is in agreement with the expected behavior for attractive interaction, where the tip is tending to pull the molecules towards the center of the detection interval.

The behavior for repulsive tip-molecule interactions is reversed: At small times $t < \tau_L$, the interaction tends to push the molecule out of the detection interval. The probability for the molecule to leave this interval at small times is thus increased compared to $\Psi_0(t)$. For larger times, $\Psi(t)$ decreases more rapidly than $\Psi_0(t)$, leading to significantly shorter mean residence times.

For both attractive and repulsive tip-molecule interaction, the power law ceases to be present at larger stiffness $|k|$ and the overall behavior can be effectively characterized by a single exponential decay.

IV. IMPLICATIONS FOR ESTIMATING MOLECULE DIFFUSION COEFFICIENTS AND TIP-MOLECULE INTERACTION

In this section, we first assess when a difference of RTD data is apparent for the cases with and without interaction. Secondly, we clarify whether a corresponding difference can be observed experimentally.

We start by evaluating the impact on diffusion parameters when neglecting the presence of the tip-molecule interactions. As for the parameters D_0 and ϵ in the model, we use typical values obtained in the RTD analysis of Ref. 5. There, the RTD analysis of freely moving copper

phthalocyanine molecules on the Ag(100) surface yielded $D_0 \simeq 10^{-10} \text{ cm}^2/\text{s}$ at a temperature of 222 K and L in the nm regime. The time resolution Δt was of the order of μs , resulting in $\epsilon \approx 0.1L$.

Taking $L = 1 \text{ nm}$, and setting $D_0/L^2 = 10^4 \text{ s}^{-1}$ and $\epsilon = 0.1L$, the eigenvalues λ_n and eigenfunctions $\varphi_n(x)$ are determined from Eq. (20) and Eq. (21), respectively. Using Eq. (11), RTDs for repulsive and attractive tip-molecule interactions are calculated for the two scaled stiffness values $\beta|k|L^2 = 10$ and 50 , with the coefficients a_n and b_n in Eq. (11) obtained from Eqs. (20) and (21).

The corresponding RTDs $\Psi(t)$ are shown in Fig. 3 for (a) $\beta kL^2 = 10$ and 50 (red lines), and (b) $\beta kL^2 = -10$ and -50 (blue lines). For comparison, the RTD $\Psi_0(t)$ for the non-interacting case ($k = 0$) is shown in both figures (gray lines). Clear differences between $\Psi_0(t)$ and $\Psi(t)$ are apparent for these realistic parameters.

Let us consider the red curves as representing experimental results that would have been measured in the presence of tip-molecule interactions. For evaluating the influence of these interactions on the RTD, however, the analysis is first carried out under the assumption that the tip-molecule interactions are not present. Accordingly, the expression given in Eq. (13) is fitted to the red curves, where only the two parameters $\tau_L = L^2/\pi^2 D_0$ and $\tilde{\epsilon} = \epsilon/L$ are adjusted.

We determined optimized values τ_L^{fit} and $\tilde{\epsilon}^{\text{fit}}$ by applying the method of least-squares to $\ln \Psi(t)$. The logarithm is taken because the characteristic changes of $\Psi(t)$ occur on scales covering several orders of magnitude, see Figs. 2 and 3. For both fit parameters, we specified ranges $\tau_L^{\text{min}} < \tau_L^{\text{fit}} < \tau_L^{\text{max}}$ and $\tilde{\epsilon}^{\text{min}} < \tilde{\epsilon}^{\text{fit}} < \tilde{\epsilon}^{\text{max}}$. In a self-consistency check, we verified that the fit of Eq. (13) to $\ln \Psi_0(t)$ yields exactly the input parameters, i.e. $\tau_L^{\text{fit}} = \tau_L$ and $\tilde{\epsilon}^{\text{fit}} = \epsilon/L$. The black dashed lines in

Fig. 3 are corresponding fits Ψ_0^{fit} of Eq. (13), i.e., under neglect of tip-molecule interaction, to the red lines representing experimental RTDs $\Psi(t)$ under influence of tip-molecule interaction.

For the repulsive interaction, we find that the fitting yields $\tilde{\epsilon}^{\text{fit}} = \tilde{\epsilon}_{\text{min}}$, even when further reducing the lower limit $\tilde{\epsilon}_{\text{min}}$ of the fitting range for $\tilde{\epsilon}^{\text{fit}}$. This is due to the fact that the fit under neglect of tip-molecule interaction underestimates $\Psi(t)$ for small times, as discussed above in connection with Fig. 2(a). This underestimation becomes less pronounced for smaller ϵ . However, the reduction of the underestimation upon decreasing $\tilde{\epsilon}_{\text{min}}$ is very weak and would hardly be noticeable when analysing experimental data affected by noise.

For the further analysis, we take $\tilde{\epsilon}_{\text{min}} = \tilde{\epsilon}^{\text{fit}} = 0.1$. We then obtain $\tau_L^{\text{fit}} = 6.1 \times 10^{-6}$ s and $\tau_L^{\text{fit}} = 1.7 \times 10^{-6}$ s for $\beta k L^2 = 10$ and 50, respectively. The dotted lines in Fig. 3(a) show $\Psi_0^{\text{fit}}(t)$ for these parameters. For $\beta k L^2 = 10$, the fit closely matches the red line, meaning that the tip-molecule interaction could go unnoticed. In that case one would obtain $D_0^{\text{fit}} = L^2/\pi^2\tau_L^{\text{fit}} \approx 1.7 \times 10^4 L^2/\text{s}$, which is 70% larger compared to the true value $D_0 = 10^4 L^2/\text{s}$. This shows that estimates of molecule diffusion coefficients can strongly deviate from the true value due to tip-molecule interactions, even if an acceptable fit to experimental data under neglect of these interactions is possible.

For the larger stiffness, $\beta k L^2 = 50$, the curve Ψ_0^{fit} in Fig. 3(a) does not give an acceptable match with the red curve. The RTD analysis would thus point to the presence of tip-molecule interactions. That the dashed line underestimates $\Psi(t)$ for short times and overestimates $\Psi(t)$ for intermediate times is an indicator that the tip-molecule interaction is repulsive.

For the attractive interaction, we find $\tilde{\epsilon}^{\text{fit}} = \tilde{\epsilon}_{\text{max}}$ even when further increasing the upper limit $\tilde{\epsilon}_{\text{max}}$ of the fitting range for $\tilde{\epsilon}^{\text{fit}}$. This is analogous to the situation described above for the repulsive interaction, where now we have an overestimation of $\Psi(t)$ at small times. We chose $\tilde{\epsilon}^{\text{fit}} = 0.1$. For the scaled stiffness $\beta k L^2 = -10$, the fit (dashed line) of Eq. (13) to $\Psi(t)$ (blue line) in Fig. 3(b) gives $\tau_L^{\text{fit}} = 2.0 \times 10^{-5}$ s. In contrast to the repul-

sive case for the small stiffness, however, the corresponding curve Ψ_0^{fit} does not yield a good match with $\Psi(t)$. That the dashed line underestimates $\Psi(t)$ for intermediate times is an indicator for an attractive tip-molecule interaction. For the larger scaled stiffness $\beta k L^2 = -50$, a fit of Eq. (13) to $\Psi(t)$ was not possible.

V. SUMMARY & CONCLUSIONS

In summary, we have presented a theory for including tip-molecule interactions in the analysis of RTDs obtained from tunneling current time series in STM experiments. For arbitrary interaction of finite range, a general formal solution in terms of an eigenfunction expansion is given. Explicit results are derived for an attractive and repulsive harmonic tip-molecule interaction. Characteristic changes of RTDs with the interaction strength are discussed and it shown how the presence of attractive and repulsive interactions can be identified. We have restricted our analysis here to the one-dimensional case. Extensions of our methodology to two dimensions are possible and will be addressed in forthcoming studies.

A very interesting point is the application of our theory to estimate tip-molecule interaction parameters. As mentioned in the introduction, the analysis of tunneling current time series allows one to determine the ITD in addition to the RTD. Fitting a measured ITD to theoretical predictions [5] yields an estimate of D_0 , because the ITD is not influenced by the tip-molecule interaction. With the knowledge of D_0 , fits of Eq. (11) to the RTD obtained from the same experiment can then be carried out with respect to the stiffness parameter k . This way an estimate for the sign and strength of tip-molecule interactions can be obtained.

This opens further interesting possibilities also for measuring molecule-molecule interactions when molecules can be picked up by an STM tip. DFT calculations could test the reliability of such methods in future studies.

-
- [1] P. Rahe, M. Kittelmann, J. L. Neff, M. Nimrich, M. Reichling, P. Maass, and A. Kühnle, "Tuning molecular self-assembly on bulk insulator surfaces by anchoring of the organic building blocks," *Adv. Mat.* **25**, 3948–3956 (2013).
 - [2] J. Barth, "Transport of adsorbates at metal surfaces: from thermal migration to hot precursors," *Surf. Sci. Rep.* **40**, 75–149 (2000).
 - [3] M. L. Lozano and M. C. Tringides, "Surface diffusion measurements from STM tunneling current fluctuations," *Europhys. Lett. (EPL)* **30**, 537–542 (1995).
 - [4] J. Ikonov, P. Bach, R. Merkel, and M. Sokolowski, "Surface diffusion constants of large organic molecules determined from their residence times under a scanning tunneling microscope tip," *Phys. Rev. B* **81**, 161412 (2010).
 - [5] S. Hahne, J. Ikonov, M. Sokolowski, and P. Maass, "Determining molecule diffusion coefficients on surfaces from a locally fixed probe: Analysis of signal fluctuations," *Phys. Rev. B* **87**, 085409 (2013).
 - [6] S. Hahne and P. Maass, "Diffusion Coefficients from Signal Fluctuations: Influence of Molecular Shape and Rotational Diffusion," *J. Phys. Chem. A* **118**, 2237–2243 (2014), 1312.2499.
 - [7] G. Zumofen, J. Hohlbein, and C. G. Hübner, "Recurrence and photon statistics in fluorescence fluctuation

- spectroscopy,” *Phys. Rev. Lett.* **93**, 260601 (2004).
- [8] E. Petrov and P. Schwille, “State of the art and novel trends in fluorescence correlation spectroscopy,” *Standardization and quality assurance in fluorescence measurements II*, 145–197 (2008).
- [9] K. Koynov and H.-J. Butt, “Fluorescence correlation spectroscopy in colloid and interface science,” *Curr. Opin. Colloid Interface Sci.* **17**, 377–387 (2012).
- [10] T. Motegi, H. Nabika, and K. Murakoshi, “Single-molecule observations for determining the orientation and diffusivity of dye molecules in lipid bilayers,” *Phys. Chem. Chem. Phys.* **15**, 12895–12902 (2013).
- [11] K. Steger, S. Bollmann, F. Noé, and S. Doose, “Systematic evaluation of fluorescence correlation spectroscopy data analysis on the nanosecond time scale,” *Phys. Chem. Chem. Phys.* **15**, 10435–10445 (2013).
- [12] S. Redner, *A guide to first-passage processes* (Cambridge university press, 2001).
- [13] H. Risken, *The Fokker-Planck Equation: Methods of Solution and Applications* (Springer-Verlag Berlin, 1985).
- [14] M. Abramowitz and I. Stegun, *Handbook of Mathematical Functions: With Formulas, Graphs, and Mathematical Tables*, Applied mathematics series (Dover Publications, 1965).